AD-A146 988 FREE SURFACE EFFECTS ON THE WAKE OF A FLAT PLATE(U) 1/1
NAVAL RESEARCH LAB WASHINGTON DC T F SWEAN ET AL.
08 NOV 84 NRL-MR-5426

UNCLASSIFIED F/G 20/4 NL

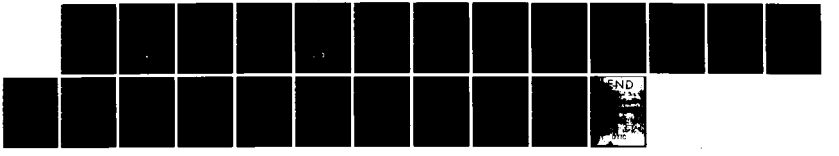

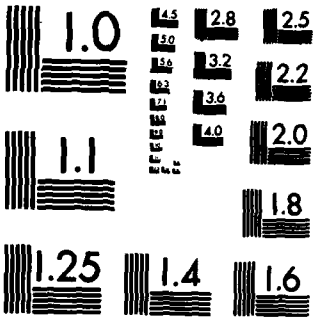
1.0
1.1
1.25
1.4
1.6
1.8
2.0
2.2
2.5
2.8
3.2
3.6
4.0
4.5
5.0
5.6
6.3
7.1

(2)

NRL Memorandum Report 5426

# Free Surface Effects on the Wake of a Flat Plate

T. F. SWEAN, JR. AND R. D. PELTZER

*Fluid Dynamics Branch*
*Marine Technology Division*

November 8, 1984



NAVAL RESEARCH LABORATORY
Washington, D.C.

SECUR. CLASSIFICATION OF THIS PAGE

## REPORT DOCUMENTATION PAGE

| | |
|---|---|
| 1a REPORT SECURITY CLASSIFICATION<br>UNCLASSIFIED | 1b. RESTRICTIVE MARKINGS |
| 2a. SECURITY CLASSIFICATION AUTHORITY | 3 DISTRIBUTION / AVAILABILITY OF REPORT<br>Approved for public release; distribution unlimited. |
| 2b DECLASSIFICATION / DOWNGRADING SCHEDULE | |
| 4 PERFORMING ORGANIZATION REPORT NUMBER(S)<br>NRL Memorandum Report 5426 | 5. MONITORING ORGANIZATION REPORT NUMBER(S) |
| 6a. NAME OF PERFORMING ORGANIZATION<br>Naval Research Laboratory<br>6b OFFICE SYMBOL (If applicable)<br>Code 5842 | 7a. NAME OF MONITORING ORGANIZATION |
| 6c. ADDRESS (City, State, and ZIP Code)<br>Washington, DC 20375-5000 | 7b. ADDRESS (City, State, and ZIP Code) |
| 8a. NAME OF FUNDING / SPONSORING ORGANIZATION<br>Office of Naval Research<br>8b. OFFICE SYMBOL (If applicable) | 9. PROCUREMENT INSTRUMENT IDENTIFICATION NUMBER |
| 8c. ADDRESS (City, State, and ZIP Code)<br>Arlington, VA 22217 | 10. SOURCE OF FUNDING NUMBERS<br>PROGRAM ELEMENT NO. 61153N; PROJECT NO.; TASK NO. RR023-01-41; WORK UNIT ACCESSION NO. EX280-250 |
| 11 TITLE (Include Security Classification)<br>Free Surface Effects on the Wake of a Flat Plate | |
| 12 PERSONAL AUTHOR(S)<br>Swean, T.F., Jr. and Peltzer, R.D. | |
| 13a. TYPE OF REPORT<br>Interim<br>13b. TIME COVERED FROM _____ TO _____ | 14. DATE OF REPORT (Year, Month, Day)<br>1984 November 8<br>15. PAGE COUNT<br>23 |
| 16 SUPPLEMENTARY NOTATION | |

| 17 COSATI CODES | | |
|---|---|---|
| FIELD | GROUP | SUB-GROUP |
| | | |
| | | |

18. SUBJECT TERMS (Continue on reverse if necessary and identify by block number)
Turbulence; Free surface; Thin shear layer equations; Wake; Spectral analysis; Turbulence model
(Continues)

19 ABSTRACT (Continue on reverse if necessary and identify by block number)

Measurements of the mean velocity and the normal and tangential stresses in the wake of a rough flat plate near a free water surface are presented. The various distributions are compared with similar measurements taken in the wake of the plate when submerged in an effectively infinite fluid. The results reveal striking differences in the manner in which the wake evolves in the two instances. In contrast to the plane wake in an infinite fluid the present experiments show that in the proximity of a free surface the wake center line (defined as the point of maximum velocity defect) migrates toward the free surface. The regions of local maxima and minima typically found in free shear layer turbulence intensity distributions also show this behavior. In addition, both the mean velocity and the turbulent fluctuations decay at a slower rate near the free surface. The implications of the experimental results regarding appropriate free surface boundary conditions for computation are discussed. The equations of continuity and momentum are solved numerically together with equations for the turbulent kinetic energy and isotropic dissipation to complete a turbulence model. The computational model is verified for the infinite wake data. Boundary conditions to simulate the free surface are
(Continues)

| | |
|---|---|
| 20 DISTRIBUTION / AVAILABILITY OF ABSTRACT<br>☒ UNCLASSIFIED/UNLIMITED ☐ SAME AS RPT ☐ DTIC USERS | 21 ABSTRACT SECURITY CLASSIFICATION<br>UNCLASSIFIED |
| 22a NAME OF RESPONSIBLE INDIVIDUAL<br>T. F. Swean, Jr. | 22b TELEPHONE (Include Area Code)<br>(202) 767-2098<br>22c. OFFICE SYMBOL<br>Code 5842 |

DD FORM 1473, 84 MAR 83 APR edition may be used until exhausted
All other editions are obsolete.

SECURITY CLASSIFICATION OF THIS PAGE

18. **SUBJECT TERMS (Continued)**

**Hot-film anemometry**, Thin shear layer equations, **Fluid mechanics**, Spectral analysis, and Turbulence model.

19. **ABSTRACT (Continued)**

**applied. The numerical results predict the major features which are observed experimentally near the free surface.** Originator-supplied Keywords include:

CONTENTS

# FREE SURFACE EFFECTS ON THE WAKE OF A FLAT PLATE

## I. INTRODUCTION

For several decades it has been realized that the presence of a free surface influences the evolution of mean velocity and turbulence but the mechanisms have not been completely described. Early observations of Nikuradse (1926) showed the flow in straight open channels to be three-dimensional and that the maximum of the streamwise mean velocity occurs below rather than coincident with the free surface. More recently, the studies of Ueda, et al. (1977) and Komori, et al. (1982) for open channel flows show that the eddy viscosity is significantly attenuated by the presence of the free surface. In the latter paper it is also shown that, near the free surface, velocity fluctuations normal to that surface are diminished while the fluctuations in the plane of the surface are increased, suggesting an overall turbulent kinetic energy preservation in that region. This paper also indicates that the viscous dissipation, $\epsilon$, has vanishingly small normal gradient near the free surface. A similar redistribution of the turbulence intensities was observed by Thomas and Hancock (1977). In their work a moving wall experiment was devised such that the wall moved at the velocity of the adjacent turbulent fluid so that no velocity gradients and shear stresses were present at the wall, conditions similar to those at a free surface. Damping of the normal velocity fluctuations and an associated increase of the longitudinal ones are observed. The spanwise fluctuations were only slightly increased. In addition the measurements of Raichlen (1967) and McQuivey and Richardson (1969), also for open channel flows, show that the macroscales of the turbulent eddies decrease considerably near the free surface. It should be pointed out that the latter two experiments do not indicate the promotion of the longitudinal turbulence intensity (the only one measured in the work of Raichlen) and the attenuation of the vertical component as in the experiments of Komori and Thomas and Hancock.

The turbulent flow in the wake of a flat plate is perhaps the simplest turbulent flow which can be realized in the laboratory. The wake is almost wholly two-dimensional and exhibits none of the transverse secondary motions present in channel flows which are to a degree responsible for some of the phenomena noted above, particularly the depression of the velocity maximum below the free surface. The study of such a flow near a free surface has the added advantage that the results can be compared with experimental data and calculations readily available in the literature for wakes in an infinite fluid. The purpose of this report is to examine the evolution of a turbulent wake produced by a flat plate near a free water surface with particular emphasis on the distributions of mean velocity, kinetic energy of turbulence, and shear stress. Wake measurements were performed in the laboratory facility described in Section II. The numerical model discussed in Section III was used to simulate and interpret the laboratory observations. The results of this study are described in Section IV, and the conclusions are presented in Section V.

## II. EXPERIMENTAL ARRANGEMENT AND PROCEDURES

The experimental program was carried out in the 1 m × 1.3 m × 18 m towing channel of the Marine Technology Division at the U.S. Naval Research Laboratory. The detailed characteristics of this facility have been described by Ramberg and Fung (1982). The towing system consists of an instrument carriage mounted on rails atop the channel sidewalls and a submerged model support carriage mounted on the channel floor. Both carriages are driven by a variable speed D.C. motor via a cable/pulley arrangement. The speed range of the towing system is 0 to 0.74 $ms^{-1}$.

Manuscript approved July 17, 1984.

The model used in these experiments was a 1 m × 0.91 m × 0.006 m aluminum flat plate which was mounted on the submerged carriage. The leading edge was tapered over the first 0.1 m for an included angle of 1.8°. The trailing edge of the plate was left blunt. The entire plate was painted with a mixture of paint and sand to promote early transition to a fully turbulent flow. No attempt was made to characterize the surface roughness in terms of equivalent sand roughness.

A rigid stainless steel probe support was connected to the instrument carriage such that it hung vertically downward at mid-span of the channel. An identical probe support was mounted near the channel sidewalls in the undisturbed fluid in order to monitor background vibration and contamination levels. Vertical location of the wake probe was controlled by means of a traversing mechanism while the plate-probe separation distance was set by individually engaging the instrument carriage and placing it in the desired location relative to the plate before the commencement of a particular measurement.

Turbulence measurements were made with DISA type 55D01 constant temperature anemometers and DISA cross-fiber-film probes type 55R61 (2 $\mu$m protective quartz coating). Probes were operated at a 1.06 overheat ratio. The anemometer outputs were linearized with DISA 55D10 linearizers and subsequently fed into a Quad Systems 721 digital recorder. Output was simultaneously monitored with an HP 5420A digital signal analyzer in order to detect abrupt probe contamination and insure the passage of starting transients before operating the digital recorder. The film probes were calibrated by moving the probes to positions outside of the wake and towing the carriage at various known velocities.

Measurements were made in the wake of the plate for four positions downstream of the trailing edge, $x/\theta_0$ = 18.6, 91.7, 244, and 438 where $\theta_0$ is the computed trailing edge momentum thickness for the infinite fluid conditions (2.53 mm). At each position vertical traverses with the hot film probe were made from a point as close to the free surface as possible to a point sufficiently below the plate to insure the determination of the wake center. Measurement points were separated in the vertical direction by 2.5 mm. For each probe-plate separation distance two flow situations were considered. In one instance the water level was maintained at 25 cm above the plate centerline in order to simulate an infinite fluid. In the second case the water depth was set to 5 cm above the plate centerline. The experimental procedure was as follows:

1. The channel was filled with ordinary tap water to a depth of 25 cm above the centerline of the flat plate. The water was then circulated through a diatomaceous earth filter for at least one day prior to the experiment. This allowed the temperature of the water to come to equilibrium with the temperature controlled environment of the laboratory while removing foreign particles which contaminate the hot-film probe.

2. The wake probe, oriented such that the sensor wires were in the vertical plane $(x,y)$ was moved to the desired vertical location and the plate-probe system was towed down the channel at a speed of 0.59 $ms^{-1}$. The carriages were then returned to the starting point and the probe moved to a new vertical location. Sufficient time was allowed to elapse between runs to insure that the water returned to a quiescent state. The probes were recalibrated after each series of runs. Each series of runs was repeated at least twice.

3. The water level was lowered to a depth of 5.0 cm above the plate and the process described in item 2 was repeated.

4. The probe was re-oriented such that the sensors were in the horizontal plane $(x,z)$ and the water depth was brought back to 25 cm. The procedures in items 1-3 were then repeated.

5. The tank was emptied of water and the probe-plate longitudinal separation was changed to prepare for a new series of experiments.

Each sensor in the cross-film probe was linearized such that for each sensor the linearizer output voltage and the flow velocity were related by

$$U_{a,b} = \gamma_{a,b} + \beta_{a,b}\, E_{a,b} \tag{1}$$

where $E$ is the linearizer output voltage and the indices $a$ and $b$ refer to sensors $a$ and $b$ of the $X$ probe. Calibration of the sensors using the method described previously yielded values for the constants $\gamma$ and $\beta$. It was found that the slopes of the calibration curves ($\beta$) changed only slightly for calibrations spaced approximately 30 minutes apart (the time allotted for a series of measurements). However, the constant $\gamma$ often changed significantly before and after an experiment, by as much as $\pm 10\%$. These calibration drifts are due to contaminants in the water. The variations in the data due to this effect are roughly: mean velocity $\pm 5\%$, turbulent kinetic energy $\pm 13\%$, and Reynolds shear stress $\pm 16\%$. The data presented in this report are the averages at each point of all the measurements taken at that point. Due to the averaging process the uncertainties in the reported data are substantially less than the variations listed above.

A second source of error in the measurements was due to the vibration of the probe due of the motion of the instrument carriage. As percentages of the towing velocity ($U_\infty$), the "apparent" rms velocities due to vibrations were typically 0.9% in the longitudinal direction (direction of tow) and 0.5% in the vertical and lateral directions. The reported results were corrected for this effect on the assumption that the turbulence and vibrational energies are statistically independent quantities. The normal turbulent stresses in the longitudinal direction, for example, were corrected according to

$$\overline{u'^2} = \overline{u_m^2} - \overline{u_b^2} \tag{2}$$

where $\overline{u_m^2}$ is the measured quantity and $\overline{u_b^2}$ is the mean square velocity fluctuation in the longitudinal direction measured outside of the wake region and is due solely to the probe motion.

## III. MODEL DESCRIPTION

### A. Mean Flow Equations

The mean velocity field of two dimension incompressible wakes is governed by the thin shear layer form of the streamwise momentum equation

$$U\frac{\partial U}{\partial x} + V\frac{\partial U}{\partial y} = -\frac{\partial}{\partial y}\left(\overline{u'v'}\right) \tag{3}$$

and by the continuity equation

$$\frac{\partial U}{\partial x} + \frac{\partial V}{\partial y} = 0 \tag{4}$$

where $U$ and $V$ are the mean flow velocities in the longitudinal ($x$) and vertical ($y$) directions respectively. Lower case letters ($u'$, $v'$) denote the fluctuating velocity components. As is usual for thin shear layers the normal stress term has been neglected in the momentum equation. The viscous stress term has also been omitted from Eq. (3) since the model will not be applied near solid walls.

### B. Turbulence Model

A turbulence model is required to determine the turbulent shear stress $\overline{u'v'}$ (actually $\overline{-\rho u'v'}$ is the shear stress) appearing in the momentum equation. The $k$-$\epsilon$ model has been shown to work well for a wide variety of flows and is discussed in detail by Rodi (1980). This model connects the shear stress to the mean velocity gradient via the eddy viscosity concept

$$\overline{-u'v'} = \nu_t \frac{\partial U}{\partial y} \tag{5}$$

and relates the kinematic eddy viscosity, $\nu_t$, to the kinetic energy of the turbulent motion, $k$, and to the rate of its dissipation, $\epsilon$, via the Kolmogorov-Prandtl expression

$$\nu_t = C_\mu \frac{k^2}{\epsilon}. \tag{6}$$

The distribution of the turbulence parameters over the flow field is obtained by solving the following semi-empirical transport equations governing these quantities:

$$U\frac{\partial k}{\partial x} + V\frac{\partial k}{\partial y} = \frac{\partial}{\partial y}\left[\frac{\nu_t}{\sigma_k}\frac{\partial k}{\partial y}\right] + \nu_t\left(\frac{\partial U}{\partial y}\right)^2 - \epsilon \tag{7}$$

$$U\frac{\partial \epsilon}{\partial x} + V\frac{\partial \epsilon}{\partial y} = \frac{\partial}{\partial y}\left[\frac{\nu_t}{\sigma_\epsilon}\frac{\partial \epsilon}{\partial y}\right] + C_1\frac{\epsilon}{k}\nu_t\left(\frac{\partial U}{\partial y}\right)^2 - \frac{C_2\epsilon^2}{k}. \tag{8}$$

In its standard form the above model contains the five constants $C_\mu$, $\sigma_k$, $\sigma_\epsilon$, $C_1$, and $C_2$ which take on the commonly accepted values of .09, 1.0, 1.3, 1.44 and 1.92 respectively.

### C. Boundary Conditions

When the edge of the wake is far removed from the free surface it is considered to be a free boundary. In this case the velocity is equal to its free stream value $U_\infty$. The ambient stream is assumed to be entirely free of turbulence so that $k$ and $\epsilon$ are zero at the free boundary.

The free surface presents considerable difficulties with respect to the correct specification of boundary conditions. In a recent paper, Naot and Rodi (1982) have surveyed much of the existing experimental work for flow involving a free surface. The three main effects observed so far pertain to open channel flows and are as follows:

1. the depression of the velocity maximum below the surface due to the nature of the secondary flows

2. the redistribution of the velocity fluctuations among the various components by damping the vertical components and enhancing the horizontal ones

3. the reduction of the eddy viscosity near the free surface presumably due to an increased dissipation brought on by a reduction of the length scale.

Naot and Rodi have proposed a model to account for these effects, the essential features of which are that $C_\mu$ is taken to be a function of the distance from the surface to account for the damping effects, and an empirical boundary condition (Dirichlet type) is invoked for $\epsilon$ at the surface to account for a reduction in length scale. All other quantities obey symmetry conditions at the free surface. Their results are in fair agreement with the experiments considered, especially with respect to the location of the velocity maximum and the eddy viscosity distribution. The computed distributions of the normal stresses do not exhibit nearly the redistribution that was present in the experiments of Komori, et al. (1982). It should be pointed out that the experiments of Raichlen (1967) and McQuivey and Richardson (1969) do not exhibit the enhancement of the longitudinal turbulence intensity at the expense of the vertical near the free surface.

An alternate and simpler approach to account for the free surface is to employ the so-called "rigid lid approximation." In this instance the surface is presumed to act as a plane of symmetry which requires $U$, $k$, and $\epsilon$ to have zero vertical gradients and $V$ to be zero at the surface. This is probably not true in all respects but the main condition of zero shear stress at the surface is simulated correctly. The major weakness is that the eddy viscosity will assume a distribution appropriate to a closed channel flow and will not display the significant reduction near the free surface which has been observed in

open channel flows. This drawback notwithstanding it is believed that the rigid lid condition is appropriate for the present study since it does not introduce additional largely untested empirical constants and functional relationships into the commonly accepted $k$-$\epsilon$ model described above and thus should more easily allow the evaluation of that model in terms of its ability to simulate the present experiments.

### D. Numerical Method

The mean flow equations together with the $k$ and $\epsilon$ equations were solved numerically with a forward marching finite difference procedure for two-dimensional boundary layer type flows described by Spalding (1977). The initial values for $U$, $k$, and $\overline{u'v'}$ were obtained from the experimental data at the first measuring station ($x/\theta_0 = 18.6$) while the distribution for the dissipation rate $\epsilon$ was obtained via Eqs. (5) and (6) where the velocity gradient was calculated from the smoothed velocity data. The numerical calculations were carried out on the Marine Technology Division HP 1000 computer. The results of the calculations are discussed in the next section.

## IV. DISCUSSION OF RESULTS

The flat plate was subjected to two different flow situations. In the first case the water level was 25 cm above the plate. During the runs the water surface remained entirely calm in the region from the leading edge of the plate to the point where the probe support pierced the water surface. This is considered to be an effectively infinite fluid since there were no surface motions and the ratio of the depth of the fluid to the wake half-width was approximately 15. In the second case (hereafter referred to as the "finite" fluid), the water level was set at 5 cm above the plate. In this situation a low amplitude transverse Kelvin wave system developed over the plate and extended downstream into the wake region. Visual observations indicated that the wave length was about 18 cm. This compares fairly well with the value of 22 cm which is predicted by the method of stationary phase (see e.g., Newman (1978)) for a point disturbance at the surface moving at the tow velocity. Measurements on the channel sidewalls of the wetted area indicated that the maximum wave amplitude was about 7 mm. This value includes all transient effects due to the starting and stopping of the carriage. Additional experiments are planned which will also examine the wave field. The discussion which follows is in three parts. First, we discuss the experimental results, primarily by distinguishing between the two flow situations described above. Second, we discuss the application of the numerical model to the data presented in the first part. In the final part we present and discuss the results of a spectral analysis of the experiment data.

### A. Experimental Results

*Infinite Fluid*

All measurements were made downstream of the centerline of the plate. The tow speed in all instances was 59 cm/s which corresponds to a Reynolds number based on plate length of $5.81 \times 10^5$. The ratio of the plate width to the wake thickness was approximately 20 so good two-dimensionality in the region away from the edges was ensured. This was confirmed by measurements of $\overline{u'w'}$ which showed that the correlation was small, indicating an absence of streamline divergence. The momentum thicknesses at each of the four stations considered were 3.42 mm, 3.23 mm, 3.12 mm, and 3.22 mm respectively. The latter three values differ by at most 3.5% while the value at the first station is about 7% greater than the average of the downstream stations. This is probably an effect due to the finite thickness of the trailing edge where a recirculating flow region is likely. That the downstream profiles exhibit essentially identical momentum thicknesses is another indication of two-dimensionality as well as the absence of longitudinal pressure gradients.

Mean flow velocities are shown in Fig. 1. The profiles possess good overall symmetry about the plate centerline with the velocity gradient at the first station being slightly higher (~8%) on the underside of the plate than on the upper. Between the first two stations it appears that the center of the wake evolves considerably more than the outer edges. This lends credence to the analysis by Alber (1980) which models the near wake as being characterized primarily by the development of an "inner" wake, a region predominantly influenced by the wall layers of the initial boundary layers. Beyond $x/\theta_0 = 91.7$ the velocity profile has evolved to a more "wakelike" appearance. The solid lines in Figs. 1-3 are representations of the numerical solution and will be discussed in a later section.

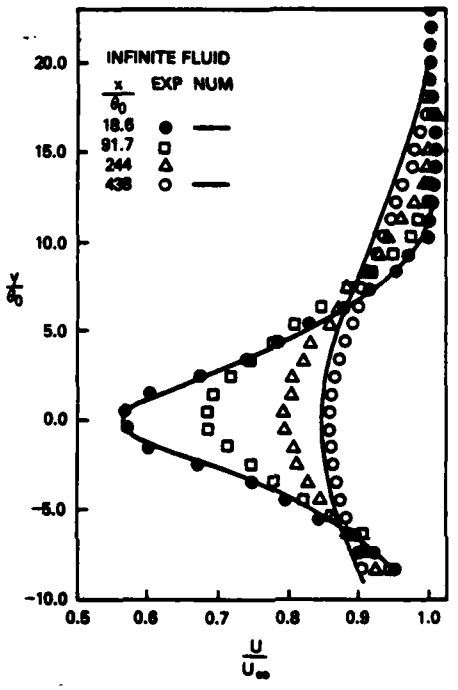


Fig. 1 — Mean velocity distribution in the infinite wake

The turbulent kinetic energy and the shear stress are shown in Figs. 2 and 3 respectively. The kinetic energy was formed from the measured values of the three normal stresses,

$$k = (\overline{u'^2} + \overline{v'^2} + \overline{w'^2})/2. \tag{9}$$

Again overall symmetry is exhibited in the profiles. Similar to the results reported by Chevray and Kovasznay (1969) these data show measurable kinetic energy significantly beyond the point where the velocity defect is zero ($y/\theta_0 \sim 18$). The point of maximum energy moves away from the plate as the distance downstream increases and occurs near the point of maximum shear.

*Finite Fluid*

The mean flow velocity distributions for the finite fluid situation are shown in Fig. 4. For purposes of comparison the infinite fluid experimental results are also shown on this figure (the dashed lines at $x/\theta_0 = 18.6$ and 438). The contrast between the two flows is evident even at the first station. The minimum velocity is about 10% less than in the infinite wake and its location has already moved a small distance (~1.5 mm) above the plate center. A larger velocity defect is observed in the entire upper half-wake and finally there is a region of velocity overshoot which is not nearly so evident for the

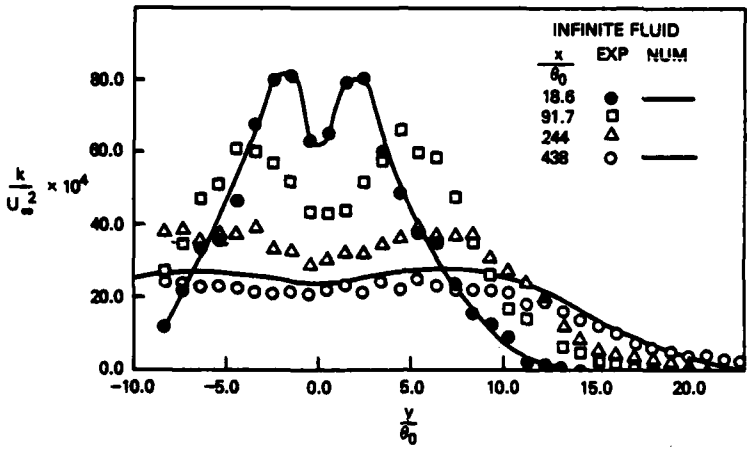


Fig. 2 — Distribution of kinetic energy of turbulence in the infinite wake

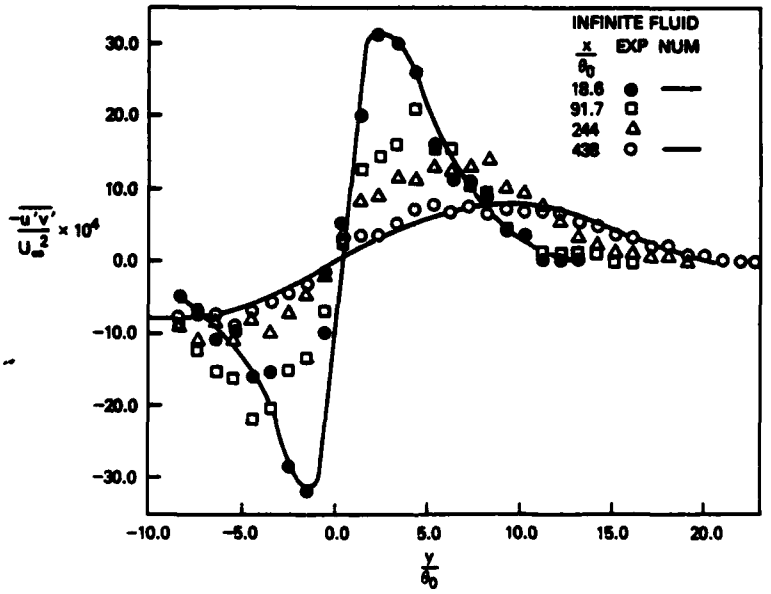


Fig. 3 — Distribution of the Reynolds shear stress in the infinite wake

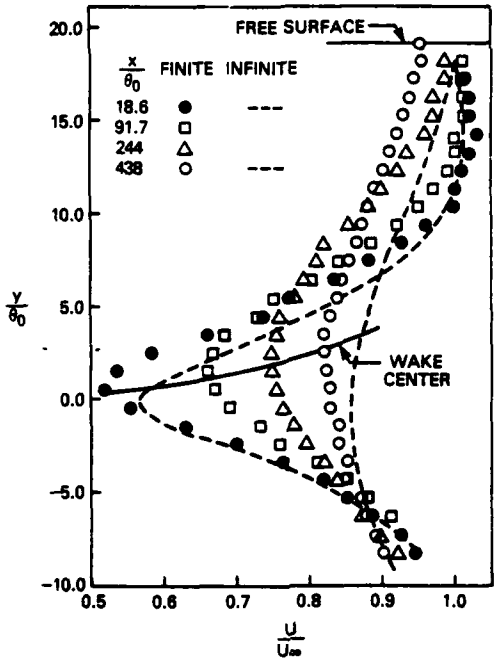


Fig. 4 — A comparison of the mean velocity distribution in the finite and infinite wakes

infinite fluid. The measured momentum thickness across the entire wake is approximately 1.05 cm versus a far downsteam value of 0.644 cm for infinite depth. Generally measurements could not be obtained closer than about 3 mm from the mean free surface. In this region probe blockage begins to be a factor as well as intermittent piercing of the free surface by the sensor. Nevertheless at the final station considered we had success in measuring very close to the surface and these results show a drag wake of approximately 5% existing at the surface. At this distance behind the plate the minimum velocity is 4% less than for the infinite fluid and it has migrated to a position nearly 7 mm ($\sim 2.5\ \theta_0$) above the plate. The estimated trajectory of the point of maximum velocity defect is shown by the solid line in Figure 4. On the other hand, in the lower half-wake there appears to be only a very gradually evolving difference between the two flows. At $x/\theta_0 = 18.6$ the profiles are essentially identical below $y/\theta_0 = -2$ whereas at $x/\theta_0 = 438$ there are significant differences until approximately $y/\theta_0 = -6$.

It is instructive to estimate the effects the Kelvin wave field may have had on the mean velocity profiles. From visual observations during the experiments the waves appeared to be steady with respect to the plate-probe system. Visual estimates yielded values of 18 cm and 7 mm for the wave length and wave amplitude respectively. The linear theory for progressive deep water waves yields the following expression for the maximum horizontal fluid velocity produced by such a wave (see e.g., Newman (1978))

$$U_W = \sqrt{2\pi g/\lambda}\, Ae^{2\pi y/\lambda} \tag{10}$$

where $\lambda$, $A$, and $g$ are the wave length, amplitude, and acceleration due to gravity respectively. The distance $y$ is measured up from the undisturbed free surface. Equation (10) is valid immediately below a crest or a trough in the wave, the velocity vector being in the direction of propagation of the wave in the first instance and opposed to it in the latter. Evaluating the above equation for the experimental conditions, one finds the wave induced motion may be as much as $\pm 22\%$ of the towing velocity very close to the free surface. As the depth increases, however, the effect is attenuated exponentially such that near the plate center ($y = -5$ cm) the effect is only about $\pm 4\%$ of the towing speed or approximately $\pm 8\%$ of the local mean velocity in that region. These approximations must be considered as

upper bounds on the wave effects. The calculation is based on a maximum wave amplitude of 7 mm obtained by observing the wetted area on the channel sidewalls subsequent to a run. A wave of this amplitude could have been transient and produced as the carriages were abruptly stopped at the end of the channel. Calculations by Wang (1984) indicate that the expected far field wave amplitude for these experimental conditions is on the order of 1 mm.

The results clearly suggest that the two flows evolved in a different manner while still on the plate. Such distinct differences in the near wake were not anticipated from preliminary theoretical considerations. The water depth was chosen such that at the operating Reynolds number the water depth was at least twice the trailing edge boundary layer thickness and in excess of 15 times the trailing edge displacement thickness. Further experiments are necessary to fully understand the flow development along the length of the plate.

The turbulent kinetic energy and shear stress are shown in Figs. 5 and 6 respectively. The mean drift toward the surface is also observed in these data. The local maxima in the kinetic energy and shear are seen to occur further from the plate on the upper side and somewhat closer on the lower side. The wake center, in this case defined by the local minimum in the kinetic energy profile, moves above the plate, a behavior observed previously for the mean velocity. This is not as obvious in the shear profiles due to the scatter in the data but a close inspection of Fig. 6 reveals that the point of zero shear stress appears to move toward the free surface. Measurable values of kinetic energy exist all the way to the free surface at the furthest downstream stations, and the data at $x/\theta_0 = 438$ tend to support a vanishing gradient for this property. The $\overline{u'v'}$ correlations extrapolate to approximately zero at the free surface as one would expect.

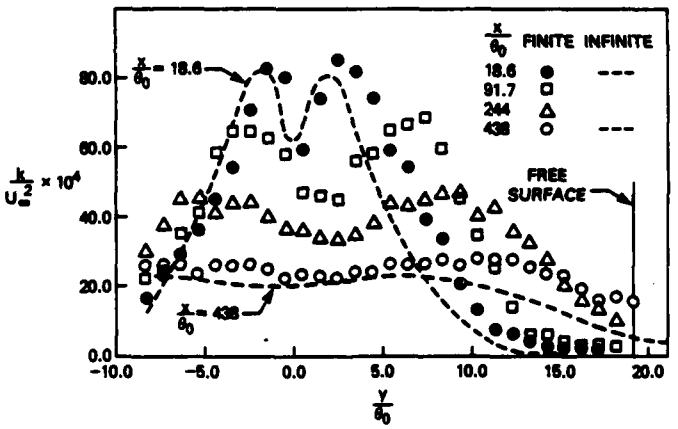


Fig. 5 — A comparison of the turbulence kinetic energy distribution in the finite and infinite wakes

Typical distributions of the longitudinal and vertical rms velocities are shown in Fig. 7. These results do not indicate the enhancement of $\overline{u^2}$ at the expense of $\overline{v^2}$ near the free surface as has been observed to occur in open channel flow by Komori, et al. (1982). These data show both components are about equally increased over their counterparts in the infinite wake. This was also true for the spanwise component ($\overline{w^2}$) which is not shown here.

There is some suggestion from the general contrast between the two flows represented in Figs. 4 through 7 that the migration of the wake might to some extent be explained by the existence of a net mean vertical velocity directed toward the surface. This could be caused for instance by a small angle

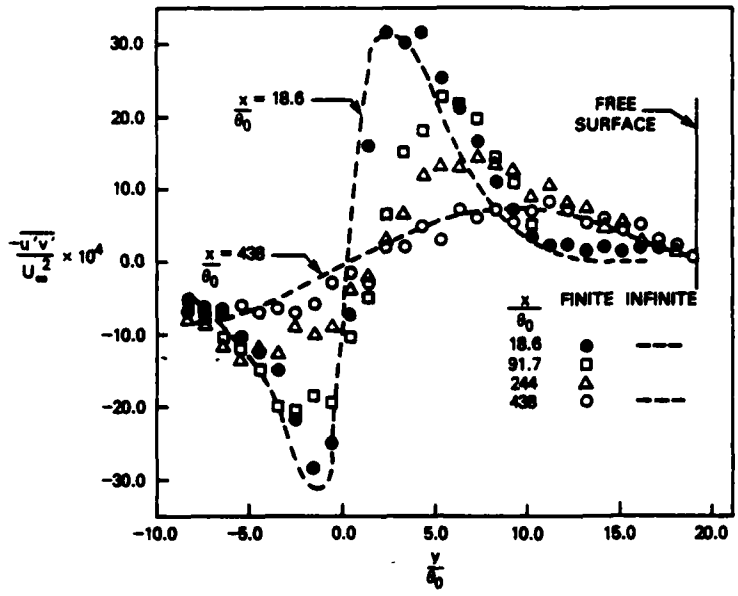


Fig. 6 — A comparison of the Reynolds shear stress distribution in the finite and infinite wakes

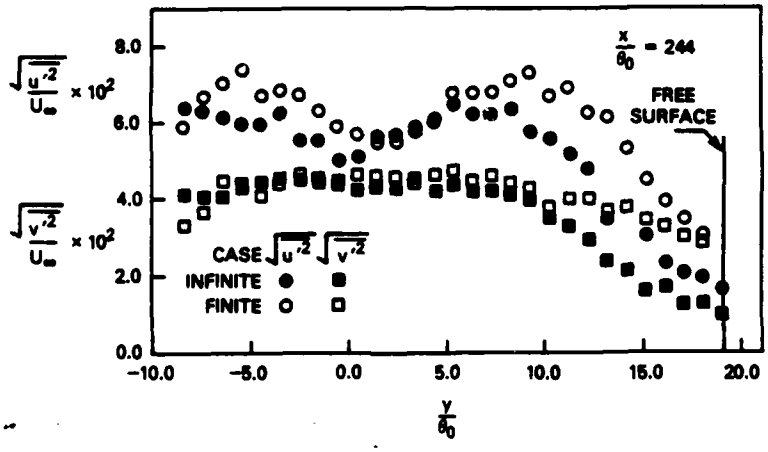


Fig. 7 — Profiles of the intensity of the streamwise and vertical velocity fluctuations in the finite and infinite wakes at $x/\theta_0 = 244$.

of attack. The net convection velocity necessary to account for the effect observed is very small, only about 0.5% of the mean flow velocity. If a net vertical velocity component of such small magnitude existed in the laboratory flow, it can not be separated from the error induced by the drift in calibration discussed in Section II. It is reassuring, however, that the profiles for the infinite wake show no tendency to drift. As is shown in the paper by Skop (1984) and also in the calculations described in the next section, a significant amount of this motion can he explained by the action of the boundary conditions imposed at the free surface.

## B. Numerical Results

The infinite wake experimental results (Figs. 1-3) are useful as a means to examine the capability of the numerical model described by Eqs. (3) through (8) to simulate a relatively fundamental

turbulent flowfield. The solid lines in these figures at $x/\theta_0 = 438$ represent the numerical solution obtained from propagating the initial conditions (solid lines at $x/\theta_0 = 18.6$) downstream. The mean velocity is underpredicted by about 1.5% throughout the wake while the calculated values of the kinetic energy are typically 15% greater than the experimental. The agreement for the shear stress is extremely good which is somewhat surprising since it is for this property that the largest data scatter was observed. Considering the overall uncertainty in the data the model is considered to perform adequately.

The experimental and calculated velocity profiles for the finite fluid wake are shown in Fig. 8. Again the initial conditions for this calculation were formed from the data at $x/\theta_0 = 18.6$. The free surface boundary conditions described in Section III were imposed at $y/\theta_0 = 19.5$. In a qualitative sense the features observed in the data are present in the numerical calculation. In this situation, however, the velocity is overpredicted by approximately 2% throughout the upper wake. The computed migration of the wake center at $x/\theta_0 = 438$ is only about half of that observed in the experiment. Similarly the drag wake existing at the free surface ($x/\theta_0 = 438$, $y/\theta_0 = 19.5$) is underpredicted by about half. The differences between the data and calculations tend to be smaller below the plate.

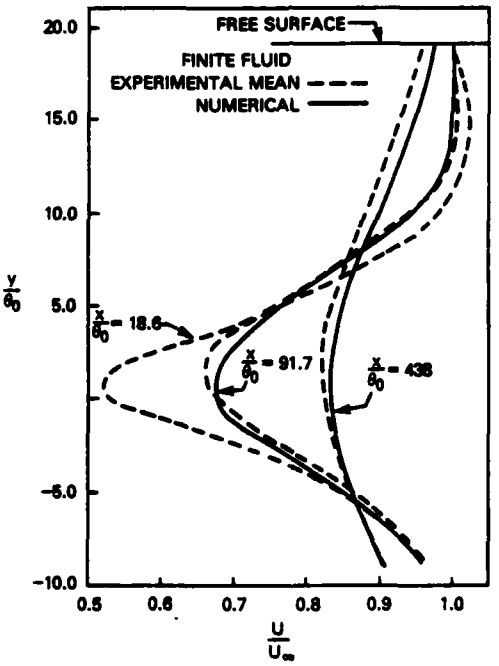


Fig. 8 — A comparison of experimental and numerical mean velocity distributions in the finite wake

Essentially the same level of agreement is achieved for the turbulent kinetic energy and shear stress shown in Figs. 9 and 10 respectively. The initial asymmetry between the lower and upper wakes is more apparent in these data. Initially the maxima of the kinetic energy and shear stress have higher values in the upper wake than in the lower. As the wake evolves the asymmetry weakens (as defined by the maximum values of the respective quantities, not the spatial distribution about the centerline) until at $x/\theta_0 = 438$ the maximum values are nearly the same in both halves of the wake. This relaxation is fairly well reproduced by the calculation although at the second station ($x/\theta_0 = 91.7$) somewhat more asymmetry is predicted. This is due to the fact that the initial velocity profile has a 20% higher gradient near the plate in the lower wake than in the upper wake (in significant contrast with the nominal 8% difference observed in the infinite wake) and therefore diffuses more rapidly in the early stages

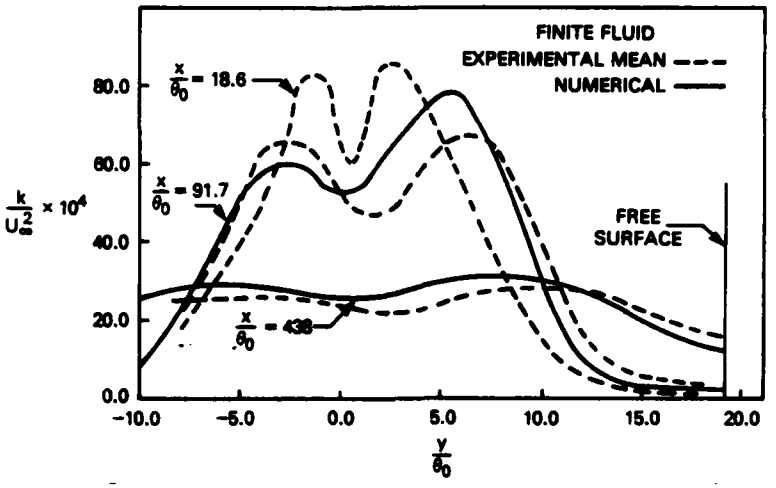


Fig. 9 — A comparison of experimental and numerical turbulence kinetic energy distributions in the finite wake

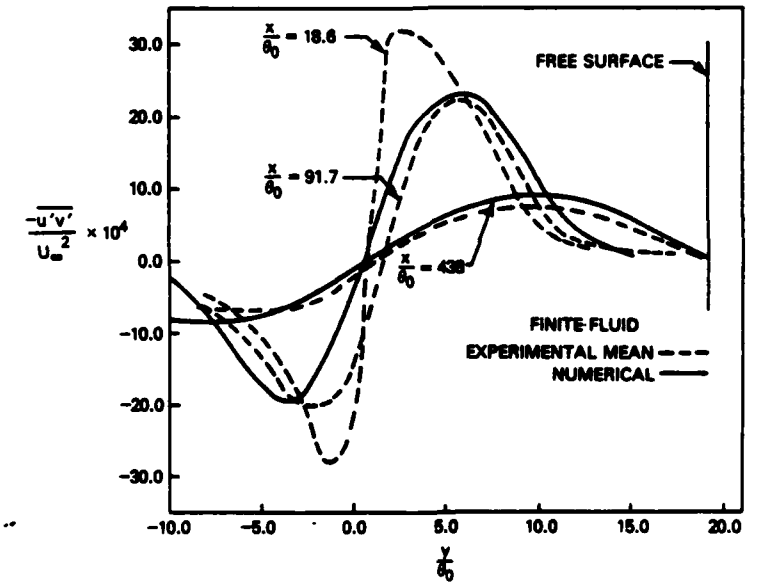


Fig. 10 — A comparison of experimental and numerical Reynolds shear stress distributions in the finite wake

of the calculation. The predicted kinetic energy near the free surface at $x/\theta_0 = 438$ is approximately 21% less than the measured value. It should be noted that the application of the wall damping functions near the free surface as proposed by Naot and Rodi (1982) would result in an increase in dissipation at the surface and therefore lower predicted values of kinetic energy which is opposite to the trend in this data (Cooper (1984)).

## C. Spectral Analysis

In the present experiments a single cross-fiber-film probe was used to obtain turbulence measurements. Consequently the space spectra can only be approximated from the computed frequency spectra assuming that the Taylor hypothesis of a frozen pattern of turbulence is valid. This hypothesis has

been shown by Lin (1953) to be fairly reasonable in the range $kL_x >> 1$ where the wave number $k$ is much larger than the reciprocal of the mean eddy size $L_x$. In the discussion which follows only the longitudinal (one-dimensional) energy spectrum will be considered.

The longitudinal energy spectrum function, $F(f)$, can be defined as

$$\int_0^\infty F(f)\,df = \overline{u'^2} \tag{11}$$

where the integration is taken over all values of the frequency $f$. The energy spectrum provides the information on how the energy is distributed with respect to the frequency. According to Kolmogoroff's theory, energy enters the spectrum through the larger eddies and is then transferred through the spectrum to the smaller eddies where it is finally dissipated. In turbulent shear flows, it is not known how the one-dimensional function is related to the three-dimensional spectrum function. However, it is assumed that the one-dimensional spectrum function is still an integral part of the three-dimensional function.

Energy spectra in regions of different mean velocity $U$ can best be compared when expressed in terms of wave number, rather than frequency. The wave number is

$$k = \frac{2\pi f}{U} \tag{12}$$

This leads to

$$F(k) = \frac{U}{2\pi} F(f) \tag{13}$$

where again Taylor's hypothesis is accepted. The frequency spectrum was obtained by the F.F.T. method and transformed into the space spectrum on the basis of Taylor's hypothesis. Finally the result was normalized into the one-dimensional wave number spectrum by dividing by the local turbulence intensity. In this case $F(k)$ satisfies

$$\int_0^\infty F(k)\,dk \approx \int_0^{k_\infty} F(k)\,dk = 1 \tag{14}$$

where $k_\infty$ is the maximum wave number which can be analyzed.

Typical energy spectra along the wake centerline for the infinite wake are shown in Fig. 11. The curves are obtained by drawing smooth curves through the computed points. The actual data are shown for $x/\theta_0 = 438$ to indicate the typical scatter. In all cases, the major energy content is in the low wave number (large eddy) range. The measurements show that there is a region $1 < k < 10$ where the one-dimensional spectrum function is proportional to $k^{-5/3}$. This indicates an ultimate decay in the inertial subrange as suggested by Kolmogoroff. At the larger wave numbers the spectra increase in slope, never quite reaching a slope of $-7$ which is predicted in the spectral region where viscous effects are important. The spectra in the higher wave number range is somewhat contaminated by the background vibration levels. At these frequencies the amplitude of the probe vibration was an unknown function of probe position and thus the signal could not be entirely removed from the data. In the low and intermediate wave number ranges ($k < 10$) the background vibrations were independent of probe location and could be removed from the data.

The Eulerian time scales can be obtained from the autocorrelation coefficient.

$$R(\tau) = \frac{\overline{u'(t)u'(t+\tau)}}{\overline{u'^2}} \tag{15}$$

The time macroscale is given by the integral,

$$T_e = \int_0^\infty R(\tau)\,d\tau \tag{16}$$

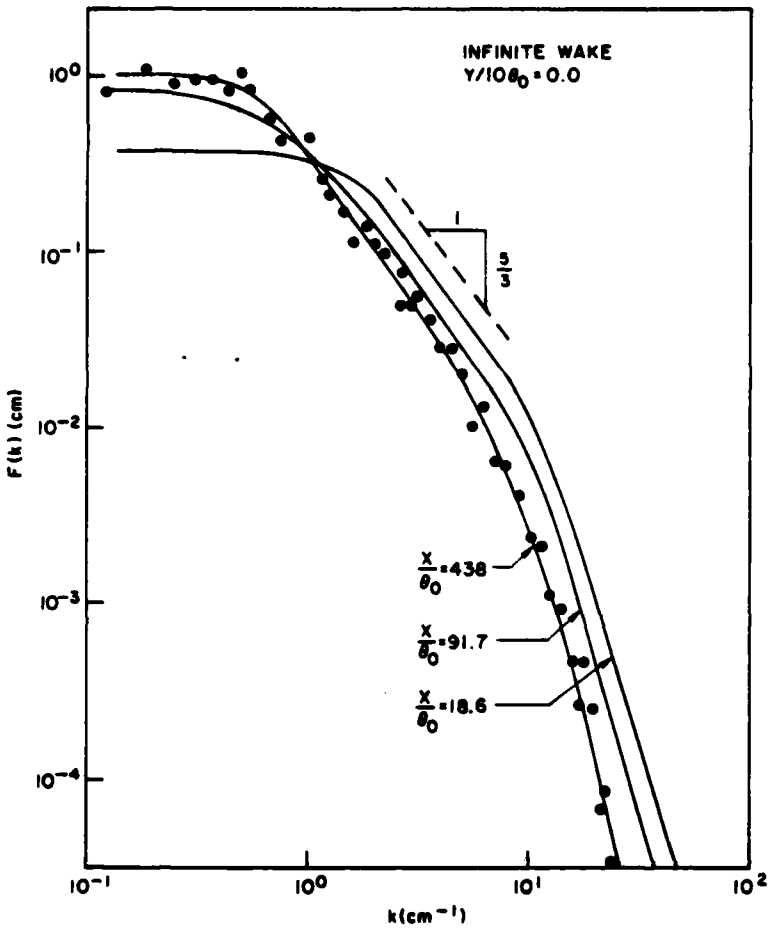


Fig. 11 — Wave number spectra along the wake centerline for the infinite wake

whereas the time microscale is obtained from the intercept of the parabolic approximation of $R(\tau)$ at small $\tau$ (see e.g., Hinze (1975)):

$$\tau_e^{-2} = \lim_{\tau \to 0} \frac{1 - R(\tau)}{\tau^2}. \tag{17}$$

Because of trends in the digital results and difficulty in determining the radius of curvature of the autocorrelation curves, the time scales were obtained from the energy spectra. As shown by Dryden, et al. (1937), the energy spectrum density and the autocorrelation function are Fourier transforms of each other. The time scales can then be obtained from the energy spectrum through the relationships

$$\tau_e^{-2} = \frac{U^2}{2} \int_0^\infty F(k) k^2 dk \tag{18}$$

and

$$T_e = \frac{\pi}{2U} \lim_{k \to 0} F(k). \tag{19}$$

The macroscale, $L_x$, an indication of the mean eddy size in the flow direction, and the microscale, $\lambda_x$, which gives a measure of the smallest eddies ultimately responsible for the dissipation of energy can then be approximated with Taylor's frozen turbulence hypothesis as

$$L_x = T_e U = \frac{\pi}{2} \lim_{k \to 0} F(k) \tag{20}$$

and

$$\lambda_x = \tau_e U = \sqrt{2}\left[\int_0^\infty F(k)k^2 dk\right]^{-1/2}. \tag{21}$$

In practice, since the spectra are only resolved down to a wave number $k \approx .2$, the interpolation formula given by Kármán (1948) and discussed fully by Hinze (1975) is employed in approximating $F(k)$ at low wave numbers. The Kármán formula may be written as,

$$F(k) = \frac{2}{\pi} L_x \{1 + (k/k_0)^2\}^{-5/6} \tag{22}$$

where $k_0$ is a characteristic wave number such that $L_x k_0 \approx 1$. Figure 12 shows the energy spectra in the finite wake at $x/\theta_0 = 18.6$ for two different $y$ locations. Also shown are the results of evaluating Eq. (22) where the macroscale is determined as that value which causes the curves to best fit the data. This figure demonstrates that the Kármán formula adequately models the spectra at low wave numbers.

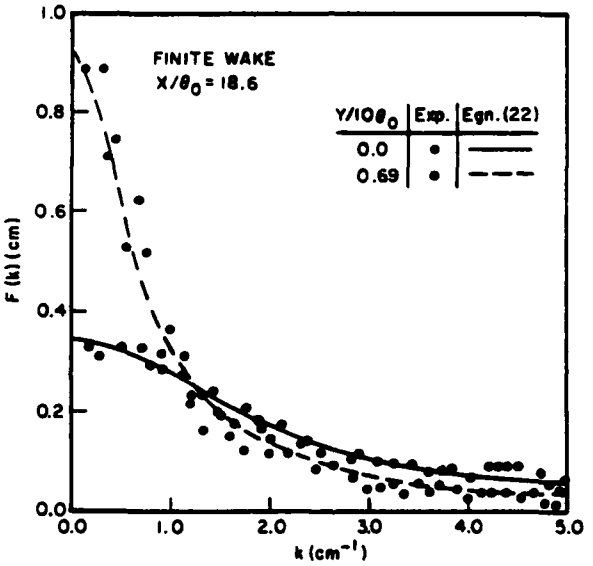


Fig. 12 — Typical wave number spectra for the finite wake at $x/\theta_0 = 18.6$

The macroscales of turbulence obtained by fitting Eq. (22) to the energy spectra are shown in Fig. 13. At any given $y$ location the macroscales increase with distance downstream of the plate in a manner consistent with the spread of the wake. At any given longitudinal station the scales increase away from the wake centerline and approach approximately constant values in the high shear region ($y > 5\theta_0$). This behavior is expected since it is well known that a diffusion length dependent only upon the longitudinal coordinate serves well to model the mean flow in planar turbulent wakes. The microscales, shown in Fig. 14, exhibit similar behavior. These data show no definitive trends which distinguish between the scales of the finite and infinite wakes, especially considering the approximate nature of their computation. Only at the final two longitudinal stations is the wake sufficiently developed to approach the free surface. At the last station ($x/\theta_0 = 438$) the macroscale tends to decrease as the free surface is approached whereas for the infinite wake the length scale remains essentially constant.

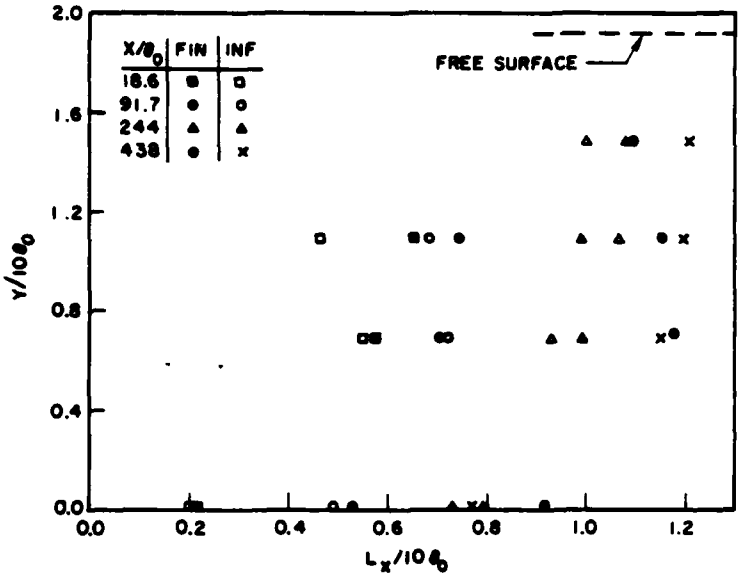


Fig. 13 — Distribution of the longitudinal macroscales in the finite and infinite wake

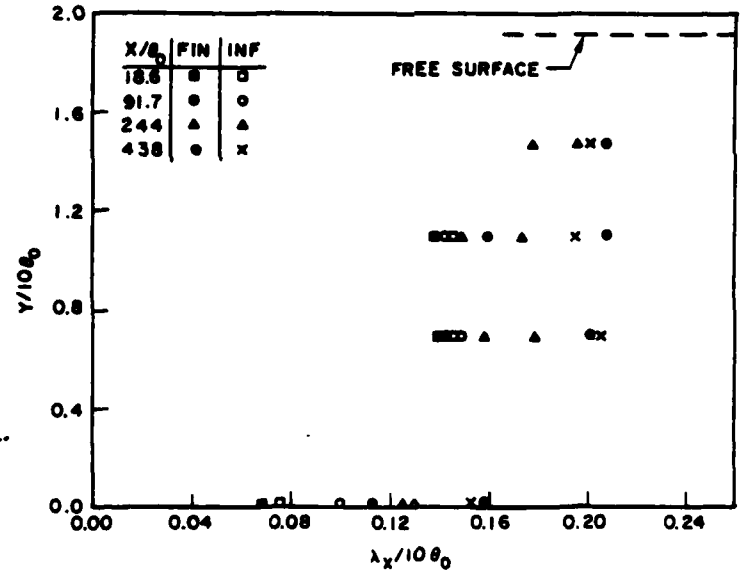


Fig. 14 — Distribution of the longitudinal microscales in the finite and infinite wake

## V. SUMMARY

The results of experiments to study the wake of a flat plate near a free water surface have been described. The evolution of the wake as defined by the distributions of mean velocity, kinetic energy of turbulence, and Reynolds shear stress was contrasted to the wake produced by the plate when in an infinite fluid. Significant differences in the two flows were observed even in the near wake region extending to over 400 momentum thicknesses downstream. The near wake velocity profile exhibits a greater velocity defect and the kinetic energy and shear stress have generally higher values when compared to the infinite wake. These changes may be due to a 'blockage' effect of the nearby free surface upon the flow over the plate. As the wake evolves downstream a slow migration toward the surface

occurs. A redistribution of kinetic energy among the various components due to surface damping effects was not observed although probe blockage effects may have obscured such a result. A spectral analysis was performed on the data in order to estimate the length scales present in the turbulent field. The macroscales and microscales increase with distance downstream of the plate trailing edge. At a given longitudinal station the scales increase with vertical distance from the wake centerline approaching nearly constant values in the high shear region. Only at the furthest longitudinal station did the macroscales of turbulence appear to significantly differ in the two flow fields considered. In this instance the macroscale in the finite wake tends to decrease as the surface is approached while that for the infinite wake remains essentially constant.

Calculations were made using a two-equation turbulence model with symmetry plane boundary conditions at the free surface. The numerical solution reproduces the observed features of the flow field qualitatively.

The results of the study to this point indicate the need for additional experiments to document the flow development along the plate and to determine the influence of the Kelvin wave field.

## VI. REFERENCES


Alber, I.E., (1980), "Turbulent Wake of a Thin, Flat Plate," AIAA J., Vol. 18, No. 9, pp. 1044-1051.

Chevray, R. and Kovasznay, L.S.G., (1969), "Turbulence Measurements in the Wake of a Thin Flat Plate," AIAA J., Vol. 7, No. 8, pp. 1641-1643.

Cooper, A.L., (1984), "Turbulent Wake of a Submerged Flat Plate," NRL Memorandum Report in preparation.

Hinze, J.O., (1975), *Turbulence*, McGraw-Hill, New York.

Kármán, T., (1948), "Progress in the Statistical Theory of Turbulence," Proc. of N.A.S., Vol. 34, pp. 530-539.

Komori, S., et al., (1982), "Turbulence Structure and Transport Mechanism at the Free Surface in an Open Channel Flow," Int. J. Heat Mass Transfer, Vol. 25, No. 4, pp. 513-521.

Lin, C.C., (1953), "On Taylor's Hypothesis and the Acceleration Terms in the Navier-Stokes Equations," Quarterly of Applied Mathematics, Vol. 10, pp. 295-306.

McQuivey, R.S. and Richardson, E.V., (1969), "Some Turbulence Measurements in Open-Channel Flow," J. of the Hydraulics Division, ASCE, Vol. 95, No. HY1, pp. 209-223.

Naot, D. and Rodi, W., (1982), "Calculation of Secondary Currents in Channel Flow," J. of the Hydraulics Division, ASCE, Vol. 108, No. HY8, pp. 948-968.

Newman, J.N., (1977), *Marine Hydrodynamics*, MIT Press, Cambridge, Massachusetts.

Nikuradse, J., "Turbulente Strömung im Innern des rechteckigen offenen Kanals," Forschungsarbeiten, Heft 281, pp. 36-44.

Raichlen, F., (1967), "Some Turbulence Measurements in Water," J. of the Engineering Mechanics Division, ASCE, Vol. 93, No. EM2, pp. 73-97.

Ramberg, S.E. and Fung, Y.T., (1982), "A New Stratified Towing Channel at NRL," NRL Memorandum Report No. 4829.

Rodi, W., (1980), *Turbulence Models and Their Application in Hydraulics*, International Association for Hydraulic Research, Delft, the Netherlands.

Skop, R.A., (1984), "The Development of Plane and Initially Axisymmetric Laminar Wakes Generated by Bodies Moving beneath a Free Surface," Computational Methods and Experimental Measurements, Proc. of the Second Int. Conference, June, 1984.

Spalding, D.B., (1977), *GENMIX: A General Computer Program for Two-dimensional Parabolic Phenomena*, Pergamon Press, New York.

Thomas, N.H. and Hancock, P.E., (1977), "Grid Turbulence Near a Moving Wall," J. Fluid Mech., Vol. 82, Pt. 3, pp. 481-496.

Ueda H., et al., (1977), "Eddy Diffusivity Near the Free Surface of Open Channel Flow," Int. J. Heat Mas Transfer, Vol. 20, No. 11, pp. 1127-1136.

Wang, H.T., (1984), Private communication.